Spectral properties of disordered Ising superconductors with singlet and triplet pairing in in-plane magnetic fields

Stefan Ilić,[1,2] Julia S. Meyer,[3] and Manuel Houzet[3]

[1]*Department of Physics and Nanoscience Center, University of Jyväskylä, P.O. Box 35 (YFL), FI-40014 University of Jyväskylä, Finland*

[2]*Centro de Física de Materiales (CFM-MPC), Centro Mixto CSIC-UPV/EHU, 20018 Donostia-San Sebastián, Spain*

[3]*Université Grenoble Alpes, CEA, Grenoble INP, IRIG, PHELIQS, 38000 Grenoble, France*

(Received 4 August 2023; revised 18 October 2023; accepted 17 November 2023; published 6 December 2023)

We study the spectral properties of disordered superconducting transition metal dichalcogenide monolayers, known as Ising superconductors, subjected to in-plane magnetic fields. In addition to the conventional singlet pairing, we also consider the recently proposed equal-spin triplet pairing, which couples to the singlet at finite in-plane magnetic fields. While both singlet and triplet order parameters are immune to intravalley scattering, they are significantly affected by intervalley scattering. In the realistic regime of strong intrinsic Ising spin-orbit coupling, we find that the properties of the superconductor are well described by a simple formula reminiscent of the well-known Abrikosov-Gor'kov theory, but with a modified self-consistency condition. Our results enable straightforward self-consistent calculation of singlet and triplet order parameters and the density of states of disordered Ising superconductors, which can be particularly useful for interpreting recent tunneling spectroscopy experiments in these systems. We also investigate the high-energy features in the density of states, the so-called mirage gaps, and discuss how they are modified by triplet pairing.

DOI: 10.1103/PhysRevB.108.214510

I. INTRODUCTION

The interplay of superconductivity and spin-dependent fields enables a plethora of exotic phenomena which provide a basis for the emerging fields of superconducting spintronics [1] and topologically protected quantum computing [2]. In the last few years, one of the key platforms for studying such phenomena has been transitional metal dichalcogenide monolayers (TMDs) [3–15]. These materials are a family of atomically thin superconductors which host strong intrinsic Ising spin-orbit coupling (ISOC) [16–18]. ISOC acts as an effective out-of-plane Zeeman field with opposite orientations at the $\pm\mathbf{K}$ corners of the Brillouin zone (valleys). ISOC has remarkable repercussions in superconducting TMDs—it strongly pins the spins of Cooper pairs to out-of-plane orientation, making TMD superconductors exceptionally robust to in-plane magnetic fields, as experimentally confirmed in various TMDs [3–5,9,10].

In addition to the conventional singlet pairing, it was recently suggested that TMD superconductors can also support unconventional equal-spin triplet pairing [19–21]. The dominant singlet order parameter can couple to the triplet order parameter at finite magnetic fields, which significantly affects the high-field behavior of the superconductor. In a recent tunneling spectroscopy experiment [15], finite triplet pairing was invoked to explain the fact that the superconducting gap was more robust to high magnetic fields than expected from the model with singlet pairing only.

Another interesting characteristic of Ising superconductors is the appearance of the so-called "mirage" gaps [22]—high-energy features in the density of states (DoS). These gaps present an experimental signature of unconventional equal-spin triplet correlations enabled by the interplay of ISOC and an in-plane Zeeman field. Finite triplet pairing provides an additional source of such correlations [15], which can modify the width of the mirage gaps [23].

Disorder plays an important role in the properties of Ising superconductors [20,24,25]. Both the singlet and equal-spin triplet order parameter are found to be immune to intravalley scattering. On the other hand, both are significantly affected by intervalley scattering. This type of disorder requires a large momentum transfer ($\sim\mathbf{K}$), and therefore it can come from sharp defects in the crystal lattice or edges of the sample. Intervalley scattering acts as an effective spin-flip mechanism which breaks Cooper pairs, namely, electrons scattered from one valley to the other "feel" opposite orientations of the Zeeman field. Moreover, since equal-spin triplet pairing is odd under change of valley, it is fully suppressed by moderate intervalley disorder.

In this work, using the quasiclassical Eilenberger formalism, we establish a theory of spectral properties of disordered Ising superconductors with mixed singlet-triplet pairing subject to in-plane Zeeman fields. For the most part, we will focus on the realistic regime of strong ISOC $\Delta_{so} \gg \Delta, \tau_{iv}^{-1}$, where Δ_{so} is the energy associated with ISOC, Δ is the superconducting gap, and τ_{iv}^{-1} is the intervalley scattering rate. This regime is relevant for most experimentally available Ising superconductors: $\Delta_{so} \gg \Delta$ holds in all superconducting TMDs, while the value of τ_{iv}^{-1} is sample dependent, but can be estimated as $\tau_{iv}^{-1} \lesssim \Delta$ in high-quality samples [15]. In this regime, we show that the quasiclassical description of Ising superconductors acquires a particularly simple form, resembling the well-known Abrikosov-Gor'kov (AG) theory [26] with a modified self-consistency condition. Our theory provides a straightforward framework for self-consistent calculation of order parameters and the DoS, which can be

particularly useful in interpretation of recent experiments such as tunneling spectroscopy measurements [7,15]. We also investigate the mirage gaps at high energies, where our AG-like description does not apply. We discuss how the mirage gaps are modified in the presence of triplet pairing, generalizing the results of Ref. [23] to the disordered case.

The paper is organized in the following way. In Sec. II we introduce the model for disordered Ising superconductors with mixed singlet and triplet pairing. In Sec. III we formulate the quasiclassical Eilenberger equation for this system. In Sec. IV we present the main result of our work—the AG-like equations describing Ising superconductors in the realistic regime of strong ISOC. We use this result to calculate self-consistent order parameters, upper critical field, and the DoS at low energies. Finally, in Sec. V, we investigate the mirage gaps by calculating the DoS at higher energies.

II. MODEL

The conduction/valence band in the normal state of disordered atomically thin two-dimensional TMDs is described by the following Hamiltonian [24,27] (see Appendix A for derivation):

$$H = \sum_{\mathbf{q}\mathbf{q}'} a^\dagger_{\mathbf{q}} \left(\mathcal{H}^N_{\mathbf{q}} \delta_{\mathbf{q}\mathbf{q}'} + \mathcal{H}^D_{\mathbf{q}\mathbf{q}'}\right) a_{\mathbf{q}'}. \tag{1}$$

Here, $a_{\mathbf{q}}=(a_{\mathbf{q}\uparrow 1}, a_{\mathbf{q}\downarrow 1}, a_{\mathbf{q}\uparrow \bar{1}}, a_{\mathbf{q}\downarrow \bar{1}})^T$ are the creation operators in the conduction/valence band with momentum $\mathbf{q}$, spin $s = \uparrow, \downarrow$, and at valley $\eta = \pm 1$. The low-energy band structure of TMDs is captured by the term

$$\mathcal{H}^N_{\mathbf{q}} = \xi_{\mathbf{q}} + \Delta_{so}\eta_z s_z + h s_x. \tag{2}$$

The Hamiltonian (2) is derived starting from a more complicated Dirac-like Hamiltonian [17,18] and projecting it to the conduction/valence band assuming a large chemical potential [24,27], as detailed in Appendix A. Here, $\xi_{\mathbf{q}} = \pm E_{\mathbf{q}} - \mu$, where $E_{\mathbf{q}} = \sqrt{q^2 v^2 + E_g^2}$ is the Dirac dispersion of TMDs [17], $\mathbf{q}$ is the small deviation of the momentum from Dirac points $\eta\mathbf{K}$, v is the velocity associated with the linearized kinetic dispersion, E_g is the difference in on-site energy responsible for opening the band gap, and μ is the chemical potential. We use units where $\hbar = k_B = 1$. The upper and lower sign in the expression for $\xi_{\mathbf{q}}$ correspond to the conduction and valence band of TMDs, respectively, which is relevant for the description of n-doped (MoS_2 [3,4], WS_2 [9]) and p-doped ($NbSe_2$ [5], TaS_2 [10]) TMD superconductors, respectively. Δ_{so} is the energy associated with ISOC, $h = g\mu_B B/2$ is related to the amplitude of the in-plane magnetic field B and the in-plane g-factor (μ_B is the Bohr magneton), and s_i and η_i ($i = x, y, z$) are Pauli matrices in the spin and valley space, respectively. Note that we neglect the contribution of the Γ point [5,10] and trigonal warping [18] in our model. Random spin-independent disorder is accounted for by the term $\mathcal{H}^D_{\mathbf{q}\mathbf{q}'}$, which contains both the intravalley scattering (with an associated scattering time τ_0) and intervalley scattering (with a scattering time τ_{iv}). In Appendix A we provide the explicit form of the disorder potential.

We consider local superconducting pairing potentials driven by a conventional mechanism of electron-phonon interaction. The Cooper pairs are formed from electrons at opposite momenta, and they necessarily come from different valleys. The superconducting order parameter can then be generally written as

$$\Psi = \Delta + \mathbf{d}\cdot\boldsymbol{s}, \tag{3}$$

where Δ is the singlet order parameter, $\mathbf{d} = (d_x, d_y, d_z)$ is a vector of the triplet order parameters, and $\mathbf{s}$ is a vector of spin Pauli matrices. The general superconducting pairing Hamiltonian is then

$$H^\Psi = \sum_{\eta\mathbf{q}ss'} [is_y\Psi]_{ss'} a^\dagger_{\mathbf{q}s\eta} a^\dagger_{\bar{\mathbf{q}}s'\bar{\eta}} + \text{H.c.}, \tag{4}$$

where we adopted the notation $\bar{\mathbf{q}} = -\mathbf{q}$, $\bar{\eta} = -\eta$. The general pairing wave function can be written as

$$\begin{aligned}|\Phi\rangle = {}& \Delta(|\uparrow\downarrow\rangle - |\downarrow\uparrow\rangle) + d_z(|\uparrow\downarrow\rangle + |\downarrow\uparrow\rangle) \\ & + d_x(|\downarrow\downarrow\rangle - |\uparrow\uparrow\rangle) + id_y(|\downarrow\downarrow\rangle + |\uparrow\uparrow\rangle).\end{aligned} \tag{5}$$

The component d_z corresponds to opposite-spin triplets, while the components $d_{x,y}$ describe equal-spin triplets. Due to the inversion symmetry breaking, the d_z triplet may exist in Ising superconductors at zero magnetic field, and its coupling to the singlet is governed by the ratio Δ_{so}/μ. Since in our model $\mu \gg \Delta_{so}$, the d_z triplet is essentially decoupled from the singlet. Moreover, d_z is suppressed by small intravalley scattering. On the other hand, applying the Zeeman field enables equal-spin triplets. As shown in Refs. [19,20], the triplet component that is perpendicular to both the Zeeman field and the ISOC field, d_y in our notation, can couple to the singlet. This singlet-triplet coupling is governed by the ratio h/Δ_{so}, and therefore the presence of the triplet can significantly alter the properties of the superconductor at sufficiently high fields. Moreover, this triplet is immune to intravalley scattering, but since it is odd in the valley index, it is still affected by intervalley scattering. In the following, we will consider an Ising superconductor with dominant singlet pairing and a subdominant d_y triplet with a relative phase of $-\pi/2$ [19,20], parametrized as $d_y = -i\eta\psi$. Other triplets, d_x and d_z, will not be considered, as they do not significantly contribute to field-dependent properties of Ising superconductors.

III. QUASICLASSICAL EQUATIONS

If the chemical potential is sufficiently away from the band gap, so that it is the dominant energy scale, $|\mu| - E_g \gg \Delta, \psi, h, \Delta_{so}, \tau_0^{-1}, \tau_{iv}^{-1}$, the Ising superconductor can be described by the quasiclassical Eilenberger equation [20,22,25]

$$\left[(\omega_n + ihs_x)\tau_z + i\eta\Delta_{so}s_z + \Delta\tau_y - \eta\psi s_y\tau_x + \frac{1}{2\tau_{iv}} g_{\bar{\eta}}, g_\eta\right] = 0. \tag{6}$$

Detailed derivation of Eq. (6) is provided in Appendix B. Here, the central object is the quasiclassical Green's function g_η, which is a matrix in spin and Nambu spaces, and satisfies

the normalization condition $g_\eta^2 = 1$. Moreover, τ_i $(i = x, y, z)$ are Pauli matrices spanning the Nambu space, $\omega_n = 2\pi T(n + \frac{1}{2})$ is the Matsubara frequency, and T is the temperature. The effect of intervalley disorder is captured by the last term on the left-hand side of the commutator in Eq. (6). Intravalley disorder has no effect on superconductivity and does not appear in the Eilenberger equation.

Using Eq. (6) and the normalization condition, we find that the quasiclassical Green's function can be parametrized by only two parameters, x and y, such that

$$g_\eta = x\left[1 + iy\tau_x - i\eta\frac{\Delta_{so}\frac{\omega_n y-\Delta}{h} - \psi}{\omega_n + \frac{x}{\tau_{iv}}\left(1 - \frac{(\omega_n y-\Delta)^2}{h^2}\right)}s_y\tau_y\right]\left[\tau_z + i\frac{\omega_n y - \Delta}{h}s_x\tau_y\right], \tag{7}$$

where x and y are determined by solving the coupled nonlinear equations

$$0 = \left[\omega_n + \frac{x}{\tau_{iv}}\left(1 - \frac{(\omega_n y - \Delta)^2}{h^2}\right)\right][(\omega_n y - \Delta)(\Delta y + \omega_n) + h^2 y] - \left(\Delta_{so}\frac{\omega_n y - \Delta}{h} - \psi\right)[(\omega_n y - \Delta)\psi - h\Delta_{so}], \tag{8}$$

$$1 = x^2\left[1 + y^2 + \left(\frac{(\omega_n y - \Delta)(\Delta y + \omega_n) + h^2 y}{(\omega_n y - \Delta)\psi - h\Delta_{so}}\right)^2\right]\left(1 - \frac{(\omega_n y - \Delta)^2}{h^2}\right). \tag{9}$$

The parameter x describes the normal part of the Green's function [component $x\tau_z$ in Eq. (7)], while the parameter y describes the singlet anomalous part [component $xy\tau_y$ in Eq. (7)]. All other components of g_η can be expressed in terms of x, y, and other model parameters, as shown in Eq. (7).

Using Eq. (7), we can write the coupled self-consistency conditions for the singlet and triplet order parameters as

$$\begin{aligned}\Delta &= \frac{\pi T g_s}{4}\sum_{\eta,\omega_n>0}\mathrm{Tr}[\tau_y g_\eta] = 2\pi T g_s\sum_{\omega_n>0} yx,\\ \psi &= \frac{\pi T g_t}{4}\sum_{\eta,\omega_n>0}\mathrm{Tr}[\eta s_y\tau_x g_\eta]\\ &= 2\pi T g_t\sum_{\omega_n>0}\frac{(\omega_n y - \Delta)(\Delta y + \omega_n) + h^2 y}{h\Delta_{so} - (\omega_n y - \Delta)\psi}x.\end{aligned} \tag{10}$$

Here, $g_{s,t} = \nu_0\lambda_{s,t}$, with the normal density of states ν_0 and the coupling constants $\lambda_{s,t}$ in the singlet and triplet channel. Density of states can be obtained after analytical continuation $i\omega_n \to \epsilon + i0^+$, where ϵ is the energy:

$$\nu(\epsilon) = \frac{\nu_0}{4}\sum_\eta \mathrm{Re}\mathrm{Tr}[\tau_z g_\eta]_{i\omega_n\to\epsilon+i0^+} = \nu_0\mathrm{Re}[x]_{i\omega_n\to\epsilon+i0^+}. \tag{11}$$

The nonlinear system of Eqs. (8) and (9) yields multiple solutions, so one needs to select the physical ones. Namely, when solving in the Matsubara frequency domain, one should choose real positive solutions $(x, y > 0)$. When solving in the energy domain, we choose the solutions yielding the positive DoS: $\mathrm{Re}[x] \geqslant 0$. In general, Eqs. (8)–(10) need to be solved simultaneously numerically, which can present a demanding computational problem. Fortunately, significant simplifications are possible in the realistic regime where spin-orbit coupling is large, which we discuss in detail in Sec. IV. For completeness, in the Appendices we present other parameter regimes where simple solutions can be found: in the absence of intervalley disorder for any ISOC strength in Appendix C, and for very strong intervalley disorder $\tau_{iv}^{-1} \gtrsim \Delta_{so} \gg \Delta$ in Appendix D.

IV. REGIME OF STRONG ISOC: $\Delta_{so} \gg \Delta, \tau_{iv}^{-1}$

In this section we focus on the realistic regime of strong ISOC. First, in Sec. IV A we present the simplified AG-like theory for this regime. These results are then used to calculate the self-consistent order parameters (Sec. IV B), upper critical field (Sec. IV C), and the DoS (Sec. IV D).

A. AG-like equation and the self-consistency condition

In the limit $\Delta_{so} \gg \tau_{iv}^{-1}, \Delta$, Eqs. (8) and (9) greatly simplify, and reduce to a single equation for the quantity $u = \Delta_{so}\rho^{-1}y^{-1}$:

$$\frac{\omega_n}{\tilde{\Delta}_{st}} = u\left(1 - \frac{\tilde{\alpha}}{\tilde{\Delta}_{st}}\frac{1}{\sqrt{1+u^2}}\right), \tag{12}$$

while $x = u/\sqrt{1+u^2}$, and we introduced $\rho = \sqrt{\Delta_{so}^2 + h^2}$. This is the Abrikosov-Gor'kov equation [26], with the depairing parameter $\tilde{\alpha}$, and a renormalized gap parameter $\tilde{\Delta}_{st}$ accounting for both singlet and triplet pairing:

$$\tilde{\alpha} = \frac{h^2}{\rho^2\tau_{iv}}, \quad \tilde{\Delta}_{st} = \frac{\Delta_{so}}{\rho}\Delta + \frac{h}{\rho}\psi. \tag{13}$$

AG theory was originally derived to describe superconductors with magnetic impurities, but its validity has since been extended to many situations where time-reversal symmetry is broken and a pair-breaking mechanism that mixes time-reversed states is present [28]. In our case, time-reversal symmetry is broken by the magnetic field, while intervalley scattering provides the pair-breaking mechanism. In most superconductors described by the AG theory, the depairing parameter is quadratic or linear in the time-reversal symmetry breaking field. In Ising superconductors, the dependence is more complex, and moreover, the renormalized gap parameter $\tilde{\Delta}_{st}$ also depends on the field.

Another difference compared to the standard AG theory is that the self-consistency condition in Ising superconductors is more complicated. The coupled self-consistency conditions (10) at temperatures smaller than the triplet critical

temperature, $T < T_{ct}$, simplify to

$$0 = \sum_{\omega_n>0}\left[\frac{1+\frac{\omega_n^2}{\omega_n^2+\rho^2}\left(\frac{\rho\Delta}{\Delta_{so}\tilde{\Delta}_{st}}-1\right)}{\sqrt{1+u^2}} - \frac{\frac{\rho\Delta}{\Delta_{so}}}{\sqrt{\omega_n^2+\Delta_0^2}}\right],$$

$$0 = \sum_{\omega_n>0}\left[\frac{1+\frac{\omega_n^2}{\omega_n^2+\rho^2}\left(\frac{\rho\psi}{h\tilde{\Delta}_{st}}-1\right)}{\sqrt{1+u^2}} - \frac{\frac{\rho\psi}{h}}{\sqrt{\omega_n^2+\psi_0^2}}\right]. \quad (14)$$

Here, Δ_0 and ψ_0 are the singlet and triplet order parameters at h, Δ_{so}, $\tau_{iv}^{-1}=0$, at the given temperature T, and we assume $\Delta_0 > \psi_0$. We used the fact that the coupling constants can be expressed as using the self-consistency condition at h, Δ_{so}, $\tau_{iv}^{-1}=0$, namely, $g_s^{-1} = 2\pi T\sum_{\omega_n}(\omega_n^2+\Delta_0^2)^{-1/2}$, while at $T<T_{ct}$ we have $g_t^{-1} = 2\pi T\sum_{\omega_n}(\omega_n^2+\psi_0^2)^{-1/2}$. On the other hand, at temperatures $T>T_{ct}$, we need to do a substitution $\sum_{\omega_n} 1/\sqrt{\omega_n^2+\psi_0^2} \to \sum_{\omega_n} 1/\omega_n - (2\pi T)^{-1}\ln T_{ct}/T$ in Eq. (14) [and also in $F(\psi_0)$ defined below]. The terms proportional to ω_n^2 in Eq. (14) must be kept to ensure convergence at high energies. Combining the two lines of Eq. (14), we can compactly write a single equation for $\tilde{\Delta}_{st}$ as

$$\frac{F(\Delta_0)F(\psi_0)}{\Delta_{so}^2F(\Delta_0)+h^2F(\psi_0)} = \sum_{\omega_n>0}\frac{1}{\sqrt{1+u^2}}\frac{1}{\omega_n^2+\rho^2}, \quad (15)$$

where we defined the function F as

$$F(x) = \sum_{\omega_n>0}\left[\frac{1}{\sqrt{1+u^2}} - \frac{\tilde{\Delta}_{st}}{\sqrt{\omega_n^2+x^2}}\right]. \quad (16)$$

If intervalley scattering is strong, $\tau_{iv}^{-1} \gg \Delta_0$, the triplet pairing is fully suppressed, and we can do the following substitutions in Eq. (12):

$$\tilde{\alpha} \to \alpha = h^2/(\Delta_{so}^2\tau_{iv}), \quad \tilde{\Delta}_{st} \to \Delta. \quad (17)$$

Moreover, the self-consistency condition in this regime simplifies to

$$\sum_{\omega_n>0}\left[\frac{1}{\sqrt{1+u^2}} - \frac{\Delta}{\sqrt{\omega_n^2+\Delta_0^2}}\right] = 0, \quad (18)$$

and at zero temperature and in the gapped regime ($\alpha<\Delta$) we have $\ln\Delta/\Delta_0 = -\alpha\pi/(4\Delta)$. Therefore, in this regime the Ising superconductor is described by the standard AG theory, with the depairing parameter quadratic in field and the standard self-consistency condition.

Equations (12) and (15) are the main results of this work, allowing for straightforward self-consistent calculations of order parameters for Ising superconductors in the realistic regime of strong ISOC. Using this result, existing AG solvers can be readily adapted for Ising superconductors with a few changes. The DoS is also readily found using our theory, as detailed in Sec. IV D.

B. Self-consistent order parameters

In Fig. 1, we show results of the self-consistent calculation of the order parameters as a function of magnetic field for different values of intervalley disorder. First, using Eqs. (12) and (15), we determine the effective order parameter $\tilde{\Delta}_{st}$, shown in Fig. 1(a). Then, using the first and second line of Eq. (14), we can separately extract the singlet and triplet order parameter, respectively, shown in Fig. 1(b). As seen from the plots, the presence of weak triplet pairing makes superconductivity significantly more robust to the effect of in-plane fields. Moreover, due to the singlet-triplet coupling by the Zeeman field, the singlet order parameter can survive far higher fields in the presence of triplets. The presence of intervalley scattering significantly reduces the upper critical field (see also Sec. IV C), and suppresses the triplet order parameter.

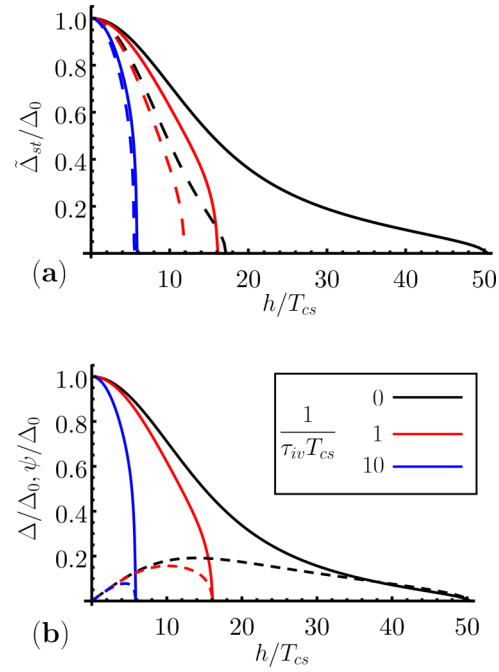

FIG. 1. (a) Renormalized order parameter $\tilde{\Delta}_{st}$ as a function of Zeeman field, for different strengths of intervalley disorder. Dashed and full lines correspond to scenarios without and with triplet pairing ($T_{ct}=0.05T_{cs}$), respectively. (b) For the scenario with triplet pairing, we plot separately the singlet and triplet order parameter, represented by the full and dashed lines, respectively. In all plots $\Delta_{so}=20T_{cs}$ and the temperature is set to $T=0.1T_{cs}$, where T_{cs} is the singlet critical temperature.

At $T=0$ and in the gapped phase ($\tilde{\alpha}<\tilde{\Delta}_{st}$), from Eq. (15) we can obtain an analytical expression determining the renormalized gap as

$$\frac{\rho^2\left(\ln\frac{\tilde{\Delta}_{st}}{\Delta_0}+\frac{\pi\tilde{\alpha}}{4\tilde{\Delta}_{st}}\right)\left(\ln\frac{\tilde{\Delta}_{st}}{\psi_0}+\frac{\pi\tilde{\alpha}}{4\tilde{\Delta}_{st}}\right)}{\Delta_{so}^2\left(\ln\frac{\tilde{\Delta}_{st}}{\Delta_0}+\frac{\pi\tilde{\alpha}}{4\tilde{\Delta}_{st}}\right)+h^2\left(\ln\frac{\tilde{\Delta}_{st}}{\psi_0}+\frac{\pi\tilde{\alpha}}{4\tilde{\Delta}_{st}}\right)} = \ln\frac{\tilde{\Delta}_{st}}{2\rho}+\frac{\pi\tilde{\alpha}}{4\tilde{\Delta}_{st}}. \quad (19)$$

In the absence of intervalley scattering, this becomes

$$\tilde{\Delta}_{st} = \Delta_0\exp\left[-\frac{h^2\ln\frac{\Delta_0}{\psi_0}\ln\frac{2\rho}{\Delta_0}}{\rho^2\ln\frac{2\rho}{\Delta_0}+\Delta_{so}^2\ln\frac{\Delta_0}{\psi_0}}\right]. \quad (20)$$

This equation illustrates that the order parameter cannot be fully suppressed by applying the Zeeman field in the absence of intervalley disorder. This means that the upper critical

field h_{c2} diverges at zero temperature, as will be discussed in Sec. IV C.

C. Upper critical field

To calculate the upper critical field h_{c2}, we use the fact that the phase transition to the normal state is of the second order [11,24], so that the order parameters vanish at the transition. Then, we may keep only the terms up to the linear order in Δ and ψ in Eqs. (12) and (14). Solving Eq. (12) yields $u = (\omega + \tilde{\alpha})/\tilde{\Delta}_{st}$, so that $1/\sqrt{1+u^2} \approx \tilde{\Delta}_{st}/(\omega+\tilde{\alpha})$. Substituting this into Eq. (14), and using that the coupling constants can be expressed in terms of singlet and triplet critical temperatures, $g_s^{-1} = 2\pi T \sum_{\omega_n} 1/\omega_n - \ln T_{cs}/T$ and $g_t^{-1} = 2\pi T \sum_{\omega_n} 1/\omega_n - \ln T_{ct}/T$, we can write the linearized gap equation as

$$\det[\hat{T} + \hat{\mathcal{S}}] = 0, \tag{21}$$

where

$$\hat{T} = \begin{bmatrix} \ln \frac{T}{T_{cs}} & 0 \\ 0 & \ln \frac{T}{T_{ct}} \end{bmatrix}, \tag{22}$$

and

$$\hat{\mathcal{S}} = \Psi\left(\frac{i\rho_{c2}}{2\pi T}\right)\frac{1}{\rho_{c2}^2}\begin{bmatrix} h_{c2}^2 & \Delta_{so}h_{c2} \\ \Delta_{so}h_{c2} & \Delta_{so}^2 \end{bmatrix} + \Psi\left(\frac{\tilde{\alpha}(h_{c2})}{2\pi T}\right)\frac{1}{\rho_{c2}^2}\begin{bmatrix} \Delta_{so}^2 & -\Delta_{so}h_{c2} \\ -\Delta_{so}h_{c2} & h_{c2}^2 \end{bmatrix}. \tag{23}$$

Here, $\Psi(x) = \mathrm{Re}[\psi(\frac{1}{2}) - \psi(\frac{1}{2}+x)]$, where $\psi(x)$ is the digamma function, and we introduced $\rho_{c2} = \sqrt{\Delta_{so}^2 + h_{c2}^2}$. Note that a more general expression for h_{c2}, valid at arbitrary Δ_{so}, has been presented in Ref. [20] (see also Appendix E).

In the absence of intervalley disorder, only the first line is finite in Eq. (23). In that case h_{c2} logarithmically diverges at zero temperature [24] in the absence of triplet pairing. The triplet pairing shifts this divergence to T_{ct}, and the critical field is infinite at all $T < T_{ct}$. At finite intervalley disorder, the depairing term in the second line of Eq. (23) cuts off the divergence. If the intervalley scattering is strong, $\tau_{iv}^{-1} \gg \Delta_0$, the triplets are fully suppressed. Moreover, in this regime $\Delta_{so} \gg h_{c2}$, so only the second line in Eq. (23) is relevant, and we obtain the standard AG depairing equation for the critical field

$$\ln \frac{T}{T_{cs}} = \Psi\left(\frac{\alpha(h_{c2})}{2\pi T}\right). \tag{24}$$

In Fig. 2, we illustrate the behavior of h_{c2} as a function of temperature at different values of intervalley scattering. We see that weak triplet pairing significantly increases the h_{c2} in the absence of intervalley disorder. Including such disorder quickly suppresses the effect of triplets.

D. Density of states

The density of states is given as

$$\nu(\epsilon) = \nu_0 \mathrm{Re}\left[\frac{u}{\sqrt{1+u^2}}\right]_{i\omega_n \to \epsilon + i0^+}, \tag{25}$$

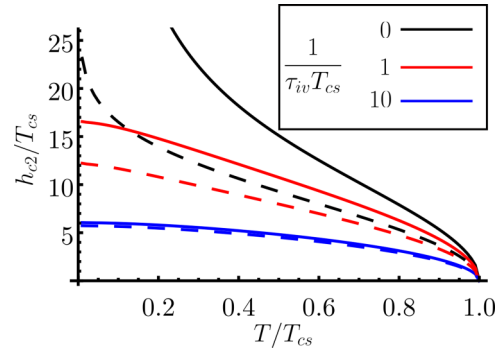

FIG. 2. Upper critical field as a function of temperature, for different values of intervalley scattering. Spin-orbit coupling is set to $\Delta_{so} = 20\,T_{cs}$. Dashed and full lines correspond to scenarios without and with triplet pairing ($T_{ct} = 0.05T_{cs}$), respectively.

where u is obtained as a solution of Eq. (12). The gap edge in the DoS is given by the standard expression [26,28]: $E_g^{2/3} = \tilde{\Delta}_{st}^{2/3} - \tilde{\alpha}^{2/3}$. Note that the DoS calculated this way is correct only at low energies, and the high-energy features of the spectrum, the "mirage" gaps, are not captured. We discuss these features in more detail in Sec. V.

In the absence of intervalley scattering, the DoS is given by sharp BCS peaks at the renormalized gap $\tilde{\Delta}_{st}$,

$$\nu(\epsilon) = \nu_0 \frac{|\epsilon|}{\sqrt{\epsilon^2 - \tilde{\Delta}_{st}^2}}\theta(|\epsilon| - \tilde{\Delta}_{st}). \tag{26}$$

In contrast to conventional superconductors, which exhibit spin splitting of the coherence peaks when the Zeeman field is applied, clean Ising superconductors will have a single coherence peak even at high fields. The only effect of increasing the field is the reduction of the gap in the quasiparticle spectrum.

Adding intervalley scattering introduces a depairing mechanism and the DoS becomes smeared [25]. In Fig. 3, we plot the DoS for different values of in-plane field, using the self-consistent order parameters from Fig. 1. As seen from the plots, the gap in the DoS is significantly more robust to the fields in the presence of triplets, due to the increased robustness of the order parameters Δ and ψ (see Fig. 1).

V. MIRAGE GAPS AT HIGH ENERGIES

Mirage gaps are high-energy half-gap features in the DoS of Ising superconductors introduced in Ref. [22] (see Fig. 4), which appear as a consequence of equal-spin triplet correlations of the form $\sim|\downarrow\downarrow\rangle + |\uparrow\uparrow\rangle$. In pure singlet-pairing Ising superconductors this type of correlation is enabled by the combination of ISOC and Zeeman field. The finite equal-spin triplet additionally contributes as a source of such correlations [15,23].

Formally, the correlations responsible for the mirage gaps are captured by the term $\sim s_y\tau_y\tau_z \sim s_y\tau_x$ in the quasiclassical Green's function g_η [see Eq. (7)]. Since these correlations are odd in valley index η, they are sensitive to intervalley disorder. This is illustrated in Fig. 4, where we show how the mirage gaps are suppressed by weak intervalley scattering.

At large ISOC, the mirage gaps appear at energies $\epsilon \approx \pm\rho$. Assuming $\Delta_{so}, \epsilon \gg \Delta_0, \tau_{iv}^{-1}, h$, from Eqs. (7) and (8) we find

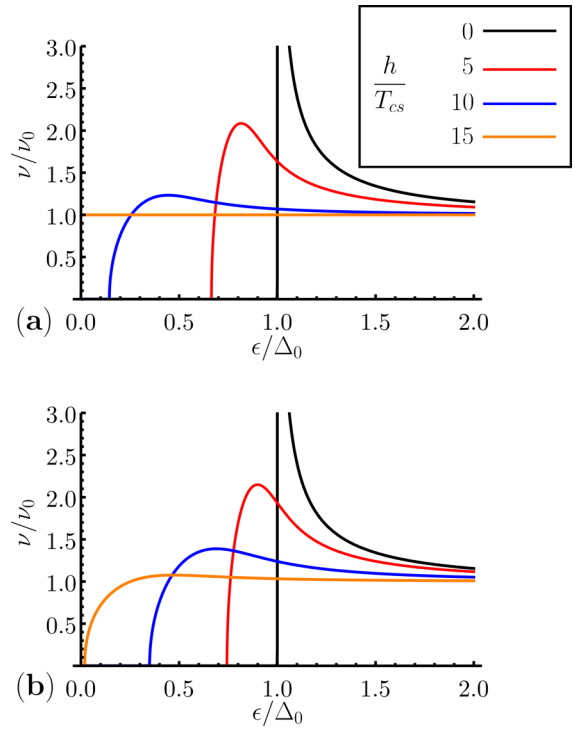

FIG. 3. Density of states of an Ising superconductor for different values of the in-plane field: (a) without triplet pairing and (b) with triplet pairing ($T_{ct} = 0.05T_{cs}$). We set $\Delta_{so} = 20\,T_{cs}$, $T = 0.1T_{cs}$, and $\tau_{iv}^{-1} = T_{cs}$. DoS is plotted using self-consistent order parameters Δ and ψ at each value of the Zeeman field (see Fig. 1).

an approximate expression for the DoS as

$$\nu \approx \frac{\nu_0}{2}\mathrm{Re}\left[1 + \frac{|\tilde{\Sigma}|}{\sqrt{\tilde{\Sigma}^2 - 4P^2}}\right]\Bigg|_{i\omega_n \to \epsilon + i0^+}, \tag{27}$$

where $\tilde{\Sigma} = \omega_n(\omega_n + \tau_{iv}^{-1}) + \rho^2 + \Delta^2 + \psi^2$ and $P = h\Delta - \Delta_{so}\psi$. In the absence of intervalley scattering, the width of the mirage gaps can be approximated as

$$W \approx \frac{2}{\rho}(h\Delta - \Delta_{so}\psi). \tag{28}$$

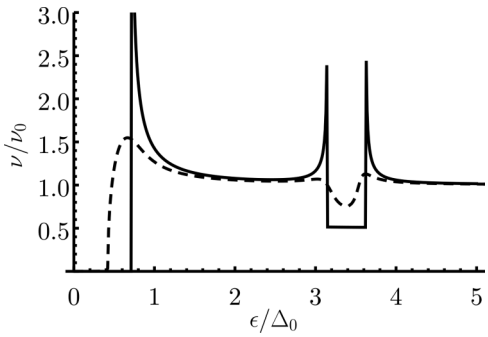

FIG. 4. Mirage gap of the Ising superconductor with triplet pairing in the absence of disorder (full line) and in the presence of weak disorder (dashed line, $\tau_{iv}^{-1} = 0.5T_{cs}$). The parameters used in the plots are $\Delta_{so} = 5T_{cs}$, $h = 3T_{cs}$, $T = 0.1T_{cs}$, and $T_{ct} = 0.05T_{cs}$.

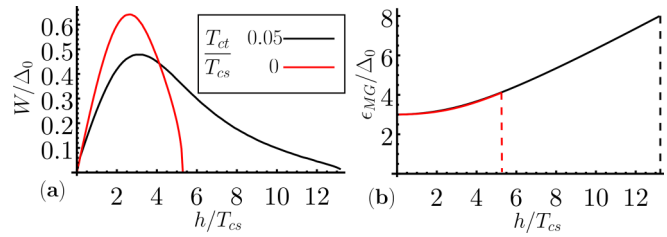

FIG. 5. (a) Width of the mirage gaps, and (b) their position, as a function of the in-plane magnetic field in the absence of intervalley disorder. We consider the scenario with and without triplet pairing ($T_{ct} = 0.05T_{cs}$). The parameters used in the plots are $\Delta_{so} = 5T_{cs}$, $T = 0.1T_{cs}$. Vertical dashed lines in (b) indicate the upper critical fields.

The ratio of the mirage gap and the main gap is then $W/(2\tilde{\Delta}_{st}) \approx h/\Delta_{so} - \rho\psi/(\Delta_{so}\tilde{\Delta}_{st})$. Therefore, the locking of the relative phase of singlet and triplet order parameters $(-\pi/2)$ is such that it increases the width of the main gap, but reduces the width of the mirage gap.

In the absence of intervalley disorder, the mirage gaps can be straightforwardly calculated at arbitrary ISOC using analytical expressions for the DoS and the self-consistency condition first presented in Ref. [15] (see also Appendix C and Ref. [23]). In Fig. 5(a), we plot the width of the mirage gap as a function of magnetic field with and without triplet pairing. At low fields, we see that the presence of triplet pairing reduces the width of mirage gaps. Moreover, in the presence of triplets the mirage gaps are able to persist up to much higher fields, due to the increased h_{c2}. These findings are consistent with the results of Ref. [23]. The position of mirage gaps ϵ_{MG}, illustrated in Fig. 5(b), is not significantly influenced by the presence of triplet pairing.

VI. CONCLUSIONS

In this work, we showed that the complex interplay of ISOC, Zeeman field, disorder, and mixed singlet-triplet pairing in Ising superconductors can be captured by relatively simple equations resembling the well-known Abrikosov-Gor'kov theory in the realistic regime of strong ISOC. We use our results to calculate the bulk properties of the superconductor such as the upper critical field and the DoS, which can be directly useful for the recent experiments measuring these quantities. Moreover, our equations could be useful for future studies of hybrid structures of Ising superconductors, such as Josephson junctions or superconductor/ferromagnet hybrids, which have recently been experimentally realized in van der Waals heterostructures [14,29,30].

ACKNOWLEDGMENTS

We thank M. Khodas and M. Haim for interesting discussions at various stages of the project. S.I. acknowledges funding from the Laboratoire d'excellence LANEF in Grenoble (Grant No. ANR-10-LABX-0051), the European Union's Horizon 2020 Research and Innovation Framework Programme under Grant No. 800923 (SUPERTED), and from the Academy of Finland Research Fellowship (Project No.

355056). J.M. acknowledges funding from the French Agence Nationale de la Recherche through Grant No. ANR-21-CE30-0035 (TRIPRES).

APPENDIX A: DIRAC-LIKE MODEL FOR TMDS AND PROJECTION TO THE CONDUCTION OR VALENCE BAND

In this Appendix, we derive the Hamiltonian (2) starting from the Dirac-like model for the normal state of TMDs [17] and projecting it to the conduction/valence band [24,27]. We also provide the explicit form of the disorder potentials for intra- and intervalley scattering in the projected basis.

The Hamiltonian describing the normal state of TMD monolayers in the vicinity of the $\pm\mathbf{K}$ points in the presence of a parallel magnetic field is given by [17,18]

$$H^N = \sum_{\mathbf{q}} c_{\mathbf{q}}^\dagger H_{\mathbf{q}}^N c_{\mathbf{q}}, \tag{A1}$$

with $H_{\mathbf{q}}^N = H_0 + H_{\rm SOC} + H_Z$, where

$$\begin{aligned} H_0 &= v(q_x\sigma_x\eta_z + q_y\sigma_y) + E_g\sigma_z, \\ H_{\rm ISOC} &= \Delta_{KM}\sigma_z\eta_z s_z + \Delta_{VZ}\eta_z s_z, \\ H_Z &= h s_x. \end{aligned} \tag{A2}$$

Here, $c_{\mathbf{q}}$=$(c_{\mathbf{q}\uparrow 1A},\ c_{\mathbf{q}\downarrow 1A},\ c_{\mathbf{q}\uparrow \bar{1}A},\ c_{\mathbf{q}\downarrow \bar{1}A},\ c_{\mathbf{q}\uparrow 1B},\ c_{\mathbf{q}\downarrow 1B},\ c_{\mathbf{q}\uparrow \bar{1}B},\ c_{\mathbf{q}\downarrow \bar{1}B})^T$ are the creation operators with momentum $\mathbf{q} = (q_x, q_y) = q(\cos\theta, \sin\theta)$ measured from $\pm\mathbf{K}$, with spin $s = \uparrow, \downarrow$, at valley $\eta = \pm 1$. Indices A and B denote d_{z^2} and $1/\sqrt{2}$ $(d_{x^2-y^2} + i\eta d_{xy})$ orbitals of the transition metal, respectively, which dominate the states in the conduction and valence band, respectively. The two Dirac cones are described by H_0. Ising spin-orbit coupling is described by $H_{\rm ISOC}$, which has two components, $\Delta_{\rm KM}$ and $\Delta_{\rm VZ}$, known as Kane-Mele and valley-Zeeman SOC, respectively. Finally, H_Z is the in-plane Zeeman field. We introduced the Pauli matrices σ_i, which span the space of transition metal d orbitals.

To proceed, we assume that H_0 gives the dominant contribution to the energy of the system. H_0 is diagonalized by the unitary transformation

$$U_{\mathbf{q}} = e^{-i\eta_z\alpha_{\mathbf{q}}}\, e^{i\beta_{\mathbf{q}}\sigma_y\eta_z}\, e^{i\alpha_{\mathbf{q}}\sigma_z\eta_z}, \tag{A3}$$

with $\tan 2\alpha_{\mathbf{q}} = q_y/q_x$, and $\tan 2\beta_{\mathbf{q}} = v|\mathbf{q}|/E_g$. It has a simple spectrum, $E_{\mathbf{q}} = \sqrt{q^2v^2 + E_g^2}$. After projecting $U_{\mathbf{q}}H_{\mathbf{q}}^N U_{\mathbf{q}}^\dagger$ onto the conduction or valence band, we obtain the effective Hamiltonian [24,27]

$$\mathcal{H}_{\mathbf{q}}^N = \xi_{\mathbf{q}} + \Delta_{so}s_z\eta_z + h s_x. \tag{A4}$$

This is Eq. (2) from the main text. Furthermore, we have introduced the spin-splitting due to ISOC,

$$\Delta_{so} = \pm\Delta_{\rm KM}\frac{E_g}{\mu} + \Delta_{\rm VZ}, \tag{A5}$$

where the upper and lower sign correspond to the projection to conduction/valence band, respectively. Here, we assumed that the chemical potential is sufficiently away from the band gap, so that it is the dominant energy scale: $|\mu| - E_g \gg \Delta_{so}, h, \Delta, \psi, \tau_0^{-1}, \tau_{iv}^{-1}$. Finally, the projected Hamiltonian (A1) can be written as

$$H^{N,p} = \sum_{\mathbf{q}} a_{\mathbf{q}}^\dagger \mathcal{H}_{\mathbf{q}}^N a_{\mathbf{q}}, \tag{A6}$$

where $a_{\mathbf{q}}$=$(a_{\mathbf{q}\uparrow 1}, a_{\mathbf{q}\downarrow 1}, a_{\mathbf{q}\uparrow \bar{1}}, a_{\mathbf{q}\downarrow \bar{1}})^T$ are the projected creation operators in the conduction/valence band, obtained using $(a_{\mathbf{q}}^c, a_{\mathbf{q}}^v)^T = U_{\mathbf{q}}c_{\mathbf{q}}$. The indices c and v, which denote the conduction and valence band, are omitted in the rest of the text for brevity.

The effect of impurities can be modeled by introducing random disorder

$$H^D = \sum_{\mathbf{q}\mathbf{q}'} c_{\mathbf{q}}^\dagger H_{\mathbf{q}\mathbf{q}'}^D c_{\mathbf{q}'}, \tag{A7}$$

with

$$H_{\mathbf{q}\mathbf{q}'}^D = V_{\mathbf{q}-\mathbf{q}'}^0 + \sum_{i=x,y} V_{\mathbf{q}-\mathbf{q}'}^i \eta_i. \tag{A8}$$

The first and second term in Eq. (A8) correspond to intra- and intervalley disorder. We characterize the disorder potentials by Gaussian correlators and assume that different kinds of disorder are uncorrelated: $\langle V_{\mathbf{q}}^i V_{\mathbf{q}'}^j\rangle_{\rm dis} = V_i^2\delta_{\mathbf{q}\bar{\mathbf{q}}'}\delta_{ij}$. Here, the brackets $\langle\ldots\rangle_{\rm dis}$ represent disorder averaging. After rotating the disorder potential, $U_{\mathbf{q}}H_{\mathbf{q}\mathbf{q}'}^D U_{\mathbf{q}'}^\dagger$, and projecting it to the conduction/valence band, we obtain the projected disorder Hamiltonian as $H^{D,p} = \sum_{\mathbf{q}\mathbf{q}'} a_{\mathbf{q}}^\dagger \mathcal{H}_{\mathbf{q}\mathbf{q}'}^D a_{\mathbf{q}'}$ with

$$\mathcal{H}_{\mathbf{q}\mathbf{q}'}^D = V_{\mathbf{q}-\mathbf{q}'}^0 f_{\theta\theta'} + \sum_{i=x,y} V_{\mathbf{q}-\mathbf{q}'}^i \tilde{f}_{\theta\theta'}\eta_i. \tag{A9}$$

Here, the functions $f_{\theta\theta'}$ and $\tilde{f}_{\theta\theta'}$ capture the anisotropy of the projected disorder potential, which is due to the momentum dependence of the unitary transformation $U_{\mathbf{q}}$ introduced in Eq. (A3). In particular, $2f_{\theta\theta'} = 1 + e^{-i\eta_z(\theta-\theta')} \pm \frac{E_g}{\mu}(1 - e^{-i\eta_z(\theta-\theta')})$ and $2\tilde{f}_{\theta\theta'} = \pm(1 - e^{-i\eta_z(\theta+\theta')}) + \frac{E_g}{\mu}(1 + e^{-i\eta_z(\theta+\theta')})$.

APPENDIX B: DERIVATION OF THE EILENBERGER EQUATION

In this Appendix we derive the Eilenberger equation (6) and the self-consistency conditions (10).

Singlet and triplet superconducting pairing potentials are described by the following Hamiltonian:

$$H^{\rm SC} = \sum_{\eta\mathbf{q}}\sum_{i=A,B}\left[\Delta c_{\mathbf{q}\uparrow\eta i}^\dagger c_{\bar{\mathbf{q}}\downarrow\bar{\eta}i}^\dagger + \psi\eta\sum_s c_{\mathbf{q}s\eta i}^\dagger c_{\bar{\mathbf{q}}s\bar{\eta}i}^\dagger\right] + \text{H.c.}. \tag{B1}$$

After projecting to the conduction/valence band (see Appendix A), this becomes

$$H^{{\rm SC},p} = \sum_{\eta\mathbf{q}}\left[\Delta a_{\mathbf{q}\uparrow\eta}^\dagger a_{\bar{\mathbf{q}}\downarrow\bar{\eta}}^\dagger + \psi\eta\sum_s a_{\mathbf{q}s\eta}^\dagger a_{\bar{\mathbf{q}}s\bar{\eta}}^\dagger\right] + \text{H.c.}. \tag{B2}$$

The mean-field singlet and triplet order parameters are determined from the self-consistency conditions

$$\Delta = -\lambda_s\sum_{\mathbf{q}\eta}\langle a_{\bar{\mathbf{q}}\downarrow\bar{\eta}}a_{\mathbf{q}\uparrow\eta}\rangle, \quad \psi = -\lambda_t\sum_{\mathbf{q}\eta s}\eta\langle a_{\bar{\mathbf{q}}s\bar{\eta}}a_{\mathbf{q}s\eta}\rangle. \tag{B3}$$

Combining the pairing Hamiltonian with the disordered normal state Hamiltonian in the projected basis we obtain $H^p = H^{N,p} + H^{D,p} + H^{\mathrm{SC},p}$, which can be rewritten as

$$H^p = \frac{1}{2}\sum_{\mathbf{q}\mathbf{q}'} \Psi^\dagger_{\mathbf{q}} \mathcal{H}^{\mathrm{BdG}}_{\mathbf{q}\mathbf{q}'} \Psi_{\mathbf{q}'}. \tag{B4}$$

Here, we introduced the Nambu pseudospinor $\Psi_{\mathbf{q}} = (a_{\mathbf{q}}\ \tilde{a}^\dagger_{\tilde{\mathbf{q}}})^T$, with $\tilde{a}^\dagger_{\tilde{\mathbf{q}}} = (a^\dagger_{\tilde{\mathbf{q}}\downarrow\tilde{1}},\ -a^\dagger_{\tilde{\mathbf{q}}\uparrow\tilde{1}},\ a^\dagger_{\tilde{\mathbf{q}}\downarrow 1},\ -a^\dagger_{\tilde{\mathbf{q}}\uparrow 1})^T$. The Bogoliubov–de Gennes (BdG) Hamiltonian is

$$\mathcal{H}^{\mathrm{BdG}}_{\mathbf{q}\mathbf{q}'} = \begin{pmatrix} \mathcal{H}^N_{\mathbf{q}}\delta_{\mathbf{q}\mathbf{q}'} + \mathcal{H}^D_{\mathbf{q}\mathbf{q}'} & (\Delta - i\psi\eta_z s_y)\delta_{\mathbf{q}\mathbf{q}'} \\ (\Delta + i\psi\eta_z s_y)\delta_{\mathbf{q}\mathbf{q}'} & -s_y\eta_x\big[\mathcal{H}^N_{\tilde{\mathbf{q}}}\delta_{\mathbf{q}\mathbf{q}'} + \mathcal{H}^D_{\tilde{\mathbf{q}}\tilde{\mathbf{q}}}\big]^T s_y\eta_x \end{pmatrix}. \tag{B5}$$

The matrix in Eq. (B5) denotes structure in the Nambu space. Using the explicit form for $\mathcal{H}^N$ and $\mathcal{H}^D$, the BdG Hamiltonian can be rewritten as $\mathcal{H}^{\mathrm{BdG}}_{\mathbf{q}\mathbf{q}'} = \mathcal{H}^{\mathrm{BdG},0}_{\mathbf{q}}\delta_{\mathbf{q}\mathbf{q}'} + \mathcal{H}^D_{\mathbf{q}\mathbf{q}'}\tau_z$, with

$$\mathcal{H}^{\mathrm{BdG},0}_{\mathbf{q}} = (\xi_{\mathbf{q}} + \Delta_{so}s_z\eta_z)\tau_z + hs_x + \Delta\tau_x + \psi\eta_z s_y\tau_y. \tag{B6}$$

Next, we introduce the Gor'kov Green's function satisfying $(i\omega_n - \mathcal{H}^{\mathrm{BdG}})G = 1$. Then, the disorder-averaged Green's function $\mathcal{G}_{\mathbf{q}} = \langle G_{\mathbf{q}\mathbf{q}'}\rangle_{\mathrm{dis}}$ can be expressed as

$$\begin{aligned} \big(i\omega_n - \mathcal{H}^{\mathrm{BdG},0}_{\mathbf{q}} - \Sigma_{\eta\mathbf{q}}\big)\mathcal{G}_{\eta\mathbf{q}} = 1, \quad \text{or} \\ \mathcal{G}_{\eta\mathbf{q}}\big(i\omega_n - \mathcal{H}^{\mathrm{BdG},0}_{\mathbf{q}} - \Sigma_{\eta\mathbf{q}}\big) = 1, \end{aligned} \tag{B7}$$

within the self-consistent Born approximation. Here, we used the fact that $\mathcal{G}_{\mathbf{q}}$ is diagonal in valley space, and $\Sigma_{\eta\mathbf{q}}$ is the self-energy associated with the disorder potential, given as

$$\Sigma_{\eta\mathbf{q}} = \sum_{\mathbf{q}'} \tau_z\big[V_0^2 F_{\theta\theta'}\mathcal{G}_{\eta\mathbf{q}'} + \big(V_x^2 + V_y^2\big)\tilde{F}_{\theta\theta'}\mathcal{G}_{\bar{\eta}\mathbf{q}'}\big]\tau_z. \tag{B8}$$

We introduced the functions $F_{\theta\theta'} = [f_{\theta\theta'}]_\eta[f_{\theta'\theta}]_\eta = \cos^2(\frac{\theta-\theta'}{2}) + \frac{E_g^2}{\mu^2}\sin^2(\frac{\theta-\theta'}{2})$, and $\tilde{F}_{\theta\theta'} = [\tilde{f}_{\theta\theta'}]_\eta[\tilde{f}_{\theta'\theta}]_{\bar{\eta}} = \frac{E_g^2}{\mu^2}\cos^2(\frac{\theta+\theta'}{2}) + \sin^2(\frac{\theta+\theta'}{2})$. The self-consistency condition (B3) can now be expressed using the Green's function as

$$\begin{aligned} \Delta &= -\frac{T\lambda_s}{4}\sum_{\mathbf{q}\eta\omega_n} \mathrm{Tr}[\tau_x\mathcal{G}_{\eta\mathbf{q}}], \\ \psi &= \frac{T\lambda_t}{4}\sum_{\mathbf{q}\eta\omega_n} \mathrm{Tr}[\eta\tau_y s_y\mathcal{G}_{\eta\mathbf{q}}]. \end{aligned} \tag{B9}$$

To proceed, we define the quasiclassical Green's function as

$$g_{\eta\theta} = \frac{i}{\pi}\int d\xi_{\mathbf{q}}\, \tau_z\mathcal{G}_{\eta\mathbf{q}}. \tag{B10}$$

After multiplying the first (second) line of Eq. (B7) by τ_z from the left (right), subtracting the two lines, and integrating over energies $\xi_{\mathbf{q}}$, we obtain the Eilenberger equation

$$[(\omega_n + ihs_x)\tau_z + i\eta\Delta_{so}s_z + \Delta\tau_y - \eta\psi s_y\tau_x + \sigma_{\eta\theta}, g_{\eta\theta}] = 0, \tag{B11}$$

where we have introduced the reduced self-energy

$$\sigma_{\eta\theta} = \pi\nu_0\int\frac{d\theta'}{2\pi}\big[V_0^2 F_{\theta\theta'}g_{\eta\theta'} + \big(V_x^2 + V_y^2\big)\tilde{F}_{\theta\theta'}g_{\bar{\eta}\theta'}\big]. \tag{B12}$$

Here, $\nu_0 = \mu/(2\pi v_F^2)$ is the normal-state density of states per valley per spin, and $v_F = v\sqrt{1 - E_g^2/\mu^2}$ is the Fermi velocity.

In order to resolve the angular structure of $g_{\eta\theta}$, we expand it into harmonics in angle θ

$$g_{\eta\theta} \approx g_\eta + g_{\eta 1}\cos\theta + g_{\eta 2}\sin\theta + \cdots. \tag{B13}$$

Then, we substitute this expansion in Eq. (B11) to obtain a system of coupled equations for the harmonics. We find that its solution yields $g_\eta \neq 0$ and $g_{\eta 1}, g_{\eta 2} = 0$. Similarly, we can show that the higher harmonics also vanish. Therefore, the quasiclassical Green's function can be taken to be independent of the angle θ and $g_{\eta\theta} = g_\eta$. Thus, the reduced self-energy simplifies to

$$\sigma_{\eta\theta} = \sigma_\eta = \frac{1}{2\tau_0}g_\eta + \frac{1}{2\tau_{iv}}g_{\bar{\eta}}. \tag{B14}$$

Here, the scattering rates are given as $\tau_0^{-1} = \pi\nu_0 V_0^2(1 + E_g^2/\mu^2)$ and $\tau_{iv}^{-1} = \pi\nu_0(V_x^2 + V_y^2)(1 + E_g^2/\mu^2)$. The particularities of scattering close to a Dirac point are not relevant in superconducting TMDs (where $|\mu| > E_g > 0$), in contrast to undoped graphene or other gapless Dirac systems (where $E_g, \mu \to 0$) [31,32]. Note that the parameters τ_0^{-1}, τ_{iv}^{-1}, ν_0, as well as v_F and Δ_{so}, are all renormalized by changing the chemical potential, via the terms proportional to E_g/μ. Placing Eq. (B14) into (B11) we finally obtain Eq. (6). Importantly, the intravalley scattering term $\frac{1}{2\tau_0}[g_\eta, g_\eta]$ vanishes, and therefore this type of disorder has no effect on superconductivity (Anderson theorem [33]).

Finally, the self-consistency condition (10) is readily obtained from (B9) after using the definition of the quasiclassical Green's function (B10).

APPENDIX C: ANALYTICAL EXPRESSIONS IN THE ABSENCE OF INTERVALLEY DISORDER AT ARBITRARY ISOC STRENGTH

In the absence of intervalley scattering, it is possible to obtain an analytical solution for the quasiclassical Green's function from Eqs. (7) and (8), without making additional assumptions about the magnitude of ISOC (see also the Supplemental Material of Ref. [15]). From there, we obtain for the DoS

$$\nu(\epsilon) = 2\nu_0\mathrm{Re}\left[\frac{\omega_n\,\mathrm{sign}(\Sigma)}{X}\left(1 + \frac{|\Sigma|}{\sqrt{\Sigma^2 - 4P^2}}\right)\right]_{i\omega_n\to\epsilon+i0^+}, \tag{C1}$$

and the coupled self-consistency conditions are

$$\Delta = 2\pi T g_s\sum_{\omega_n>0}\frac{1}{X}\left[\Delta\left(1 + \frac{\Sigma - 2h^2}{\sqrt{\Sigma^2 - 4P^2}}\right) + \psi\frac{2h\Delta_{so}}{\sqrt{\Sigma^2 - 4P^2}}\right], \tag{C2}$$

$$\psi = 2\pi T g_t\sum_{\omega_n>0}\frac{1}{X}\left[\psi\left(1 + \frac{\Sigma - 2\Delta_{so}^2}{\sqrt{\Sigma^2 - 4P^2}}\right) + \Delta\frac{2h\Delta_{so}}{\sqrt{\Sigma^2 - 4P^2}}\right]. \tag{C3}$$

We introduced the notation $\Sigma = \omega_n^2 + \rho^2 + \Delta^2 + \psi^2$, $P = h\Delta - \Delta_{so}\psi$, and $X = \sqrt{2}[\Sigma - 2\rho^2 + \text{sign}(\Sigma)\sqrt{\Sigma^2 - 4P^2}]^{1/2}$.

APPENDIX D: STRONGLY DISORDERED LIMIT $\tau_{iv}^{-1} \gtrsim \Delta_{so} \gg \Delta$

In the main text, we focused on the realistic regime of strong ISOC, $\Delta_{so} \gg \tau_{iv}^{-1}, \Delta$. Here, we will consider the opposite regime $\tau_{iv}^{-1} \gtrsim \Delta_{so} \gg \Delta$.

For strong-enough intervalley scattering, $\tau_{iv}^{-1} \gg \Delta$, triplet pairing is suppressed, as shown in the main text. In this regime, the general equations (8) and (9) reduce to

$$\frac{\omega_n \pm ih}{\Delta} = u_\pm + \frac{\Delta_{so}^2 \tau_{iv}}{2\Delta} \frac{u_\pm - u_\mp}{\sqrt{1+u_\mp^2}}, \tag{D1}$$

where $2x = \sum_\pm u_\pm (1+u_\pm^2)^{-1/2}$ and $2y = x^{-1}\sum_\pm (1+u_\pm^2)^{-1/2}$. This is equivalent to the result of Maki and Tsuneto [34] for two-dimensional superconductors with spin-orbit impurities. Namely, the effect of ISOC is fully captured by an effective spin-orbit scattering rate $\Delta_{so}^2\tau_{iv}$. Note that a similar effective scattering rate also appears in the studies of weak localization of TMD materials in the relevant regime [27].

As in Ref. [34], the DoS is given as

$$\nu(\epsilon) = \frac{\nu_0}{2}\sum_\pm \text{Re}\left[\frac{u_\pm}{\sqrt{1+u_\pm^2}}\right]_{i\omega_n \to \epsilon + i0^+}, \tag{D2}$$

the self-consistency condition is

$$\Delta = \pi T g_s \sum_{\omega_n > 0, \pm} \frac{1}{\sqrt{1+u_\pm^2}}, \tag{D3}$$

and the linearized gap equation is

$$\ln\frac{T}{T_{cs}} = 2\pi T \sum_{\omega_n}\left[\frac{1}{\omega_n} - \frac{\omega_n + \Delta_{so}^2\tau_{iv}}{h^2 + \omega_n(\omega_n + \Delta_{so}^2\tau_{iv})}\right]. \tag{D4}$$

Note that Eq. (D1) reduces to the Abrikosov-Gor'kov equation if ISOC is strong enough, $\Delta_{so}^2\tau_{iv} \gg \Delta_0$, with a depairing parameter $\alpha = h^2/(\Delta_{so}^2\tau_{iv})$ and the gap parameter Δ. Therefore, there is an overlap with the regime $\Delta_{so} \gg \tau_{iv}^{-1} \gg \Delta_0$ presented in Eqs. (17) and (18) of the main text.

On the other hand, for weak ISOC, $\Delta_{so}^2\tau_{iv} \ll \Delta_0$, we recover the standard equations for the paramagnetically limited superconductor. Here, the electrons are so frequently scattered between the valleys that they no longer "feel" the ISOC. In this regime the DoS is spin split

$$\nu(\epsilon) = \frac{\nu_0}{2}\sum_\pm \text{Re}\frac{\epsilon \pm h}{\sqrt{(\epsilon \pm h)^2 - \Delta^2}}, \tag{D5}$$

and the linearized gap equation is

$$\ln\frac{T_{cs}}{T} = \text{Re}\left[\psi\left(\frac{1}{2} + \frac{ih}{2\pi T}\right) - \psi\left(\frac{1}{2}\right)\right]. \tag{D6}$$

APPENDIX E: UPPER CRITICAL FIELD AT ARBITRARY ISOC STRENGTH

In Sec. IV B we presented an analytical result determining the upper critical field at strong ISOC $\Delta_{so} \gg \Delta, \tau_{iv}^{-1}$. Here, we will derive a more general expression valid for any ISOC strength.

In the vicinity of the transition to the normal state, we linearize Eq. (8) in order parameters and solve it to determine y by taking $x \approx 1$. Then, we can obtain the coupled linear gap equations from Eq. (10),

$$\begin{aligned}\Delta &= 2\pi T g_s \sum_{\omega_n>0}\left[\Delta\frac{\omega_n\left(\omega_n + \frac{1}{\tau_{iv}}\right) + \Delta_{so}^2}{\mathcal{A}_n} + \psi\frac{\Delta_{so}h_{c2}}{\mathcal{A}_n}\right],\\ \psi &= 2\pi T g_t \sum_{\omega_n>0}\left[\Delta\frac{\Delta_{so}h_{c2}}{\mathcal{A}_n} + \psi\frac{\omega_n^2 + h_{c2}^2}{\mathcal{A}_n}\right].\end{aligned} \tag{E1}$$

Here, we introduced $\mathcal{A}_n = (\omega_n + \frac{1}{\tau_{iv}})(\omega_n^2 + \rho_{c2}^2) - \frac{1}{\tau_{iv}}\Delta_{so}^2$. Then, the linear gap equation can be written in the form $\det[\hat{T} + \hat{\mathcal{S}}] = 0$, where $\hat{T}$ was introduced in Eq. (22), and

$$\hat{\mathcal{S}} = \begin{bmatrix}\mathcal{S}_s & \mathcal{S}_{st}\\ \mathcal{S}_{st} & \mathcal{S}_t\end{bmatrix}, \tag{E2}$$

where

$$\begin{aligned}\mathcal{S}_s &= 2\pi T\sum_{\omega_n>0}\left[\frac{1}{\omega_n} - \frac{\omega_n\left(\omega_n + \frac{1}{\tau_{iv}}\right) + \Delta_{so}^2}{\mathcal{A}_n}\right],\\ \mathcal{S}_t &= 2\pi T\sum_{\omega_n>0}\left[\frac{1}{\omega_n} - \frac{\omega_n^2 + h_{c2}^2}{\mathcal{A}_n}\right],\\ \mathcal{S}_{st} &= 2\pi T\sum_{\omega_n>0}\frac{\Delta_{so}h_{c2}}{\mathcal{A}_n}.\end{aligned} \tag{E3}$$

Similar expressions were previously reported in Ref. [20]. In the case of singlet pairing only, the linear gap equation reduces to $\ln(T_{cs}/T) = \mathcal{S}_s$ [24]. Taking the limit $\Delta_{so} \gg \Delta, \tau_{iv}^{-1}$, Eqs. (E2) and (E3) reduce to Eq. (23) from the main text.

[1] J. Linder and J. W. Robinson, Superconducting spintronics, Nat. Phys. **11**, 307 (2015).

[2] J. Alicea, New directions in the pursuit of Majorana fermions in solid state systems, Rep. Prog. Phys. **75**, 076501 (2012).

[3] J. Lu, O. Zheliuk, I. Leermakers, N. F. Yuan, U. Zeitler, K. T. Law, and J. Ye, Evidence for two-dimensional Ising superconductivity in gated MoS_2, Science **350**, 1353 (2015).

[4] Y. Saito, Y. Nakamura, M. S. Bahramy, Y. Kohama, J. Ye, Y. Kasahara, Y. Nakagawa, M. Onga, M. Tokunaga, T. Nojima *et al.*, Superconductivity protected by spin–valley locking in ion-gated MoS_2, Nat. Phys. **12**, 144 (2016).

[5] X. Xi, Z. Wang, W. Zhao, J.-H. Park, K. T. Law, H. Berger, L. Forró, J. Shan, and K. F. Mak, Ising pairing in superconducting $NbSe_2$ atomic layers, Nat. Phys. **12**, 139 (2016).

[6] Y. Xing, K. Zhao, P. Shan, F. Zheng, Y. Zhang, H. Fu, Y. Liu, M. Tian, C. Xi, H. Liu *et al.*, Ising superconductivity and quantum phase transition in macro-size monolayer $NbSe_2$, Nano Lett. **17**, 6802 (2017).

[7] T. Dvir, F. Massee, L. Attias, M. Khodas, M. Aprili, C. H. Quay, and H. Steinberg, Spectroscopy of bulk and few-layer superconducting $NbSe_2$ with van der Waals tunnel junctions, Nat. Commun. **9**, 598 (2018).

[8] D. Costanzo, H. Zhang, B. A. Reddy, H. Berger, and A. F. Morpurgo, Tunnelling spectroscopy of gate-induced superconductivity in MoS_2, Nat. Nanotechnol. **13**, 483 (2018).

[9] J. Lu, O. Zheliuk, Q. Chen, I. Leermakers, N. E. Hussey, U. Zeitler, and J. Ye, Full superconducting dome of strong Ising protection in gated monolayer WS_2, Proc. Natl. Acad. Sci. USA **115**, 3551 (2018).

[10] S. C. De la Barrera, M. R. Sinko, D. P. Gopalan, N. Sivadas, K. L. Seyler, K. Watanabe, T. Taniguchi, A. W. Tsen, X. Xu, D. Xiao *et al.*, Tuning Ising superconductivity with layer and spin–orbit coupling in two-dimensional transition-metal dichalcogenides, Nat. Commun. **9**, 1427 (2018).

[11] E. Sohn, X. Xi, W.-Y. He, S. Jiang, Z. Wang, K. Kang, J.-H. Park, H. Berger, L. Forró, K. T. Law *et al.*, An unusual continuous paramagnetic-limited superconducting phase transition in 2D $NbSe_2$, Nat. Mater. **17**, 504 (2018).

[12] J. Li, P. Song, J. Zhao, K. Vaklinova, X. Zhao, Z. Li, Z. Qiu, Z. Wang, L. Lin, M. Zhao *et al.*, Printable two-dimensional superconducting monolayers, Nat. Mater. **20**, 181 (2021).

[13] C.-w. Cho, J. Lyu, L. An, T. Han, K. T. Lo, C. Y. Ng, J. Hu, Y. Gao, G. Li, M. Huang, N. Wang, J. Schmalian, and R. Lortz, Nodal and nematic superconducting phases in $NbSe_2$ monolayers from competing superconducting channels, Phys. Rev. Lett. **129**, 087002 (2022).

[14] A. Hamill, B. Heischmidt, E. Sohn, D. Shaffer, K.-T. Tsai, X. Zhang, X. Xi, A. Suslov, H. Berger, L. Forró *et al.*, Two-fold symmetric superconductivity in few-layer $NbSe_2$, Nat. Phys. **17**, 949 (2021).

[15] M. Kuzmanović, T. Dvir, D. LeBoeuf, S. Ilić, M. Haim, D. Möckli, S. Kramer, M. Khodas, M. Houzet, J. S. Meyer *et al.*, Tunneling spectroscopy of few-monolayer $NbSe_2$ in high magnetic fields: Triplet superconductivity and Ising protection, Phys. Rev. B **106**, 184514 (2022).

[16] Z. Y. Zhu, Y. C. Cheng, and U. Schwingenschlögl, Giant spin-orbit-induced spin splitting in two-dimensional transition-metal dichalcogenide semiconductors, Phys. Rev. B **84**, 153402 (2011).

[17] D. Xiao, G.-B. Liu, W. Feng, X. Xu, and W. Yao, Coupled spin and valley physics in monolayers of MoS_2 and other group-VI dichalcogenides, Phys. Rev. Lett. **108**, 196802 (2012).

[18] A. Kormányos, G. Burkard, M. Gmitra, J. Fabian, V. Zólyomi, N. D. Drummond, and V. Fal'ko, $k \cdot p$ theory for two-dimensional transition metal dichalcogenide semiconductors, 2D Mater. **2**, 022001 (2015).

[19] D. Möckli and M. Khodas, Magnetic-field induced $s + if$ pairing in Ising superconductors, Phys. Rev. B **99**, 180505(R) (2019).

[20] D. Möckli and M. Khodas, Ising superconductors: Interplay of magnetic field, triplet channels, and disorder, Phys. Rev. B **101**, 014510 (2020).

[21] D. Wickramaratne, S. Khmelevskyi, D. F. Agterberg, and I. I. Mazin, Ising superconductivity and magnetism in $NbSe_2$, Phys. Rev. X **10**, 041003 (2020).

[22] G. Tang, C. Bruder, and W. Belzig, Magnetic field-induced mirage gap in an ising superconductor, Phys. Rev. Lett. **126**, 237001 (2021).

[23] S. Patil, G. Tang, and W. Belzig, Spectral properties of a mixed singlet-triplet Ising superconductor, Front. Electron. Mater. **3**, 1254302 (2023).

[24] S. Ilić, J. S. Meyer, and M. Houzet, Enhancement of the upper critical field in disordered transition metal dichalcogenide monolayers, Phys. Rev. Lett. **119**, 117001 (2017).

[25] M. Haim, D. Möckli, and M. Khodas, Signatures of triplet correlations in density of states of Ising superconductors, Phys. Rev. B **102**, 214513 (2020).

[26] A. A. Abrikosov and L. P. Gor'kov, Contribution to the theory of superconducting alloys with paramagnetic impurities, Zh. Eksp. Teor. Fiz. **39**, 1781 (1960) [Sov. Phys. JETP **12**, 1243 (1961)].

[27] S. Ilić, J. S. Meyer, and M. Houzet, Weak localization in transition metal dichalcogenide monolayers and their heterostructures with graphene, Phys. Rev. B **99**, 205407 (2019).

[28] K. Maki, Gapless superconductivity, in *Superconductivity* (Routledge, Boca Raton, 2018), pp. 1035–1105.

[29] H. Idzuchi, F. Pientka, K.-F. Huang, K. Harada, Ö. Gül, Y. J. Shin, L. Nguyen, N. Jo, D. Shindo, R. Cava *et al.*, Unconventional supercurrent phase in Ising superconductor Josephson junction with atomically thin magnetic insulator, Nat. Commun. **12**, 5332 (2021).

[30] K. Kang, S. Jiang, H. Berger, K. Watanabe, T. Taniguchi, L. Forró, J. Shan, and K. F. Mak, Giant anisotropic magnetoresistance in Ising superconductor-magnetic insulator tunnel junctions, arXiv:2101.01327.

[31] P. Adroguer, D. Carpentier, J. Cayssol, and E. Orignac, Diffusion at the surface of topological insulators, New J. Phys. **14**, 103027 (2012).

[32] W. Chen, Edelstein and inverse Edelstein effects caused by the pristine surface states of topological insulators, J. Phys.: Condens. Matter **32**, 035809 (2020).

[33] L. Andersen, A. Ramires, Z. Wang, T. Lorenz, and Y. Ando, Generalized Anderson's theorem for superconductors derived from topological insulators, Sci. Adv. **6**, eaay6502 (2020).

[34] K. Maki and T. Tsuneto, Pauli paramagnetism and superconducting state, Prog. Theor. Phys. **31**, 945 (1964).